IMPOSING BIAXIAL STRAIN ON 2D LAYERED MATERIALS BY LIQUID-INDUCED SWELLING OF SUPPORTING POLYMER

[1,2]Krishna SAMPATHKUMAR, [1]Jan PEKAREK, [2]Otakar FRANK

[1]CEITEC - Brno University of Technology, Brno, Czech Republic, EU,
krishna.sampathkumar@ceitec.vutbr.cz
[2]J.Heyrovsky Institute of Physical Chemistry of the CAS, Prague, Czech Republic, EU,
otakar.frank@jh-inst.cas.cz

https://doi.org/10.37904/nanocon.2020.3685

Abstract

2D layered materials promise to revolutionize the field of electronics, photonics, optoelectronics, energy storage, and sensing, etc. 2D materials have exceptional mechanical properties, with critical elongation >10%. Employing the strain to manipulate the electronic structure of these 2D materials could lead to further improvement of their implementation in many aspects. The ease of manipulation of their electronic structure can be one of the critical factors for their utilization in photonic devices. Apart from the strain, which decreases (increases) the bandgap energy at the rate of ~100 meV under 1% of biaxial tension (compression), also the layer number causes bandgap energy change of, e.g., 0.5 eV between bulk (1.3 eV) and monolayer MoS_2 (1.8 eV). In our work, we focus on using the swelling behavior of PMMA/SU8 polymer in methanol to impose the strain on 2D layered materials. In the first trials, we have shown that it is possible to reach a strain gradient from 0 to ~0.5% of biaxial strain via simple swelling of polymer substrates, both for graphene [1] and transition metal di-chalcogenides (TMDC) like MoS_2. Raman spectroscopy was used to probe the lattice strain in the materials through measuring changes of vibrational frequencies, and photoluminescence was used to probe the strain-induced bandgap character and energy in TMDC at room temperature. The surface corrugation of the 2D material after the soaking was recorded with the help of atomic force microscope (AFM).

Keywords: 2D material, graphene, TMDC, strain engineering, biaxial strain

1. INTRODUCTION

Most of the material's physical properties can be tuned via strain engineering by mechanically modifying its structure. Two-dimensional nanomaterials' unique mechanical properties are particularly promising candidates for strain engineering and related applications because they can withstand considerable strain before structural failure. The atomically thin monolayer graphene exhibits unique chemical and electronic properties. The strain in graphene can change its electronic structure, chemical potential, or induce pseudo magnetic gauge fields. Other than graphene, strain engineering offers great potential to control and modify the optoelectronic structure of transition metal dichalcogenides [1-3].

The fast-growing field of flexible devices requires more fundamental research to keep the material science to help the future application. For example, the recent growth of graphene usage in the near field communication (NFC) tags and antennae is the perfect illustration. However, the 2D materials often exhibit a change in their fundamental electrical, optical, and structural properties, requiring further studies and classifications based on their modulation in a real situation under strain/stress. The in-plane stress imposed on a 2D material can be either purely planar or can be manifested by out-of-plane buckling. The buckling patterns can have periodical tensile and compressive strains across the 2D material. Externally imposed deformation such as pressure-

induced, tip-induced, blister formation, or substrate bending are the preferential methods in the case of 2D materials [4,5].

A polymer substrate swelled with diffusing fluids can also impose strain on the material. In the present work, we show polymethylmethacrylate (PMMA) swelled by methanol [6-8] inducing large deformation in selected 2D material resting on top of it. The strain-dependent change in electronic band structure were detected through the respective characteristic peak shifts in the Raman and photoluminescence spectra (PL) graphene and TMDC flakes [9,10].

2. EXPERIMENTAL METHODS

Polymethylmethacrylate (PMMA) slabs were coated with ~500nm thick SU8 2000.5 (MicroChem) negative photoresist. The SU8-covered PMMA substrates were annealed at 60°C for 5 minutes to evaporate the solvent present in the SU8. Graphene and MoS_2 flakes were mechanically cleaved using scotch tape and directly exfoliated on the SU8-coated PMMA substrates. The exfoliated samples were prebaked at 65°C for 30 minutes to get a conformal adhesion with the SU8 surface on the PMMA slab. The exfoliated graphene and MoS_2 sample thickness were identified using optical contrast measurement in an optical microscope. Raman and PL spectroscopy were used to quantify the evolution of the biaxial strain in graphene and MoS_2.

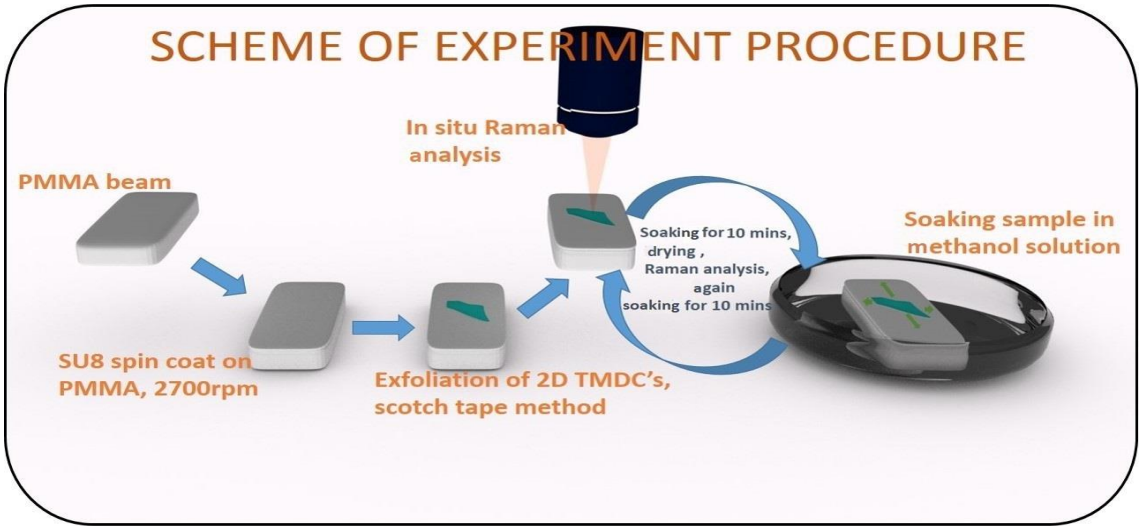

Figure 1. Schematic representation of the experiment

The biaxial strain was imposed on the 2D materials (graphene or MoS_2) by soaking in methanol in repeated ten-minute intervals [11-13]. After every soaking period (10 minutes), the samples were dried in air at room temperature before doing the Raman or PL spectral mapping. Figure 1 represents the experimental scheme. For the graphene samples, the Raman spectral mapping, and for the MoS_2 sample, both Raman and PL spectral mapping were performed with LabRAM HR (Horiba). The Raman spectra were measured using a 633nm laser excitation, and PL was measured using 532nm laser excitation, both with 600 l/mm grating. Both Raman and PL maps were recorded with a 2-micrometer (μm) step size. The atomic force microscopy (AFM) images were obtained with the Dimension Icon microscope (Bruker).

3. RESULTS AND DISCUSSION

Topographically two different graphene samples, named G1 and G2, were considered for the initial swelling experiment. The swollen SU8 imposed strain on the graphene samples, which can be quantified using the in-situ Raman spectroscopy, showing a phonon softening (blue shift) of the characteristic Raman peaks [14] [15]. The Raman 2D band, with frequency ω_{2D} ~2680cm^{-1}, was used to quantify the strain in the graphene samples

instead of the G band ω_G ~1580cm^{-1}, because the 2D band is much more sensitive than the G band to biaxial strain effects [10,16,17]. The AFM topography (**Figure 1e**) shows a large flake with a high level of structural uniformity. The color-coded ω_{2D} map in **Figure 1 a-e** shows the evolution of the imposed strain for the soaking intervals of 10 minutes. The localized tensile strain in the graphene flake's center region received the maximum interfacial stress transfer from the polymer swelling (to ~2510 cm^{-1}, corresponding to 0.5 % of biaxial strain) after 40 minutes of soaking time. After that, the stress transfer between the polymer and graphene G1 failed.

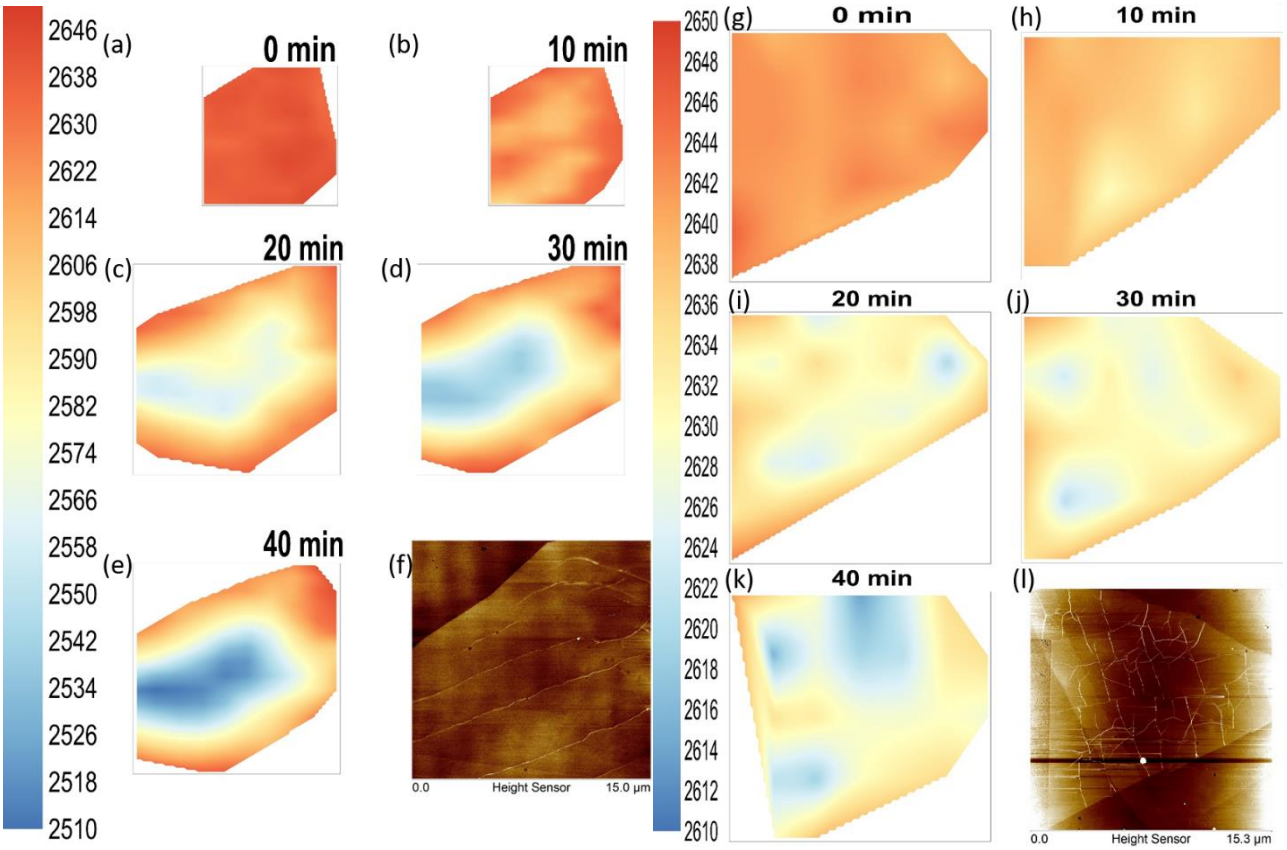

Figure 1. Evolution of Raman spectral features of monolayer graphene samples G1 and G2. (a-e), (g-k) show the Raman 2D band shift for different soaking times, in G1, and G2, respectively. (f), (l) the AFM topography images of G1 and G2, respectively, before soaking.

In the same fashion, the topography of sample G2 was recorded before the soaking experiment. Sample G2 has more cracks, which separate the graphene into fragments of lateral dimension between 1-3 µm. **Figure 1 g-k** shows the color-coded Raman spectral maps of the 2D peak for the time intervals of 10 minutes. The imposed strain is not homogenous across the sample. The interfacial stress is very low in the small graphene domains, which results in the small and random strain in the sample G2. Although SU8 and graphene have an excellent interfacial stress transfer, the graphene grain boundaries restrict reaching such high strain levels as in the sample G1. The ω_{2D} and soaking time correlation plot, **Figure 2**, statistically compares the results from the two samples. **Figure 2** proves that smaller strain was imposed on the sample G2 compared to the sample G1. The median of the ω_{2D} shift reached in sample G1 corresponded to ~0.5%, and the maximum to more than 1% [18,19].

In the sample G2, less than 0.1% strain was achieved by the swelling experiment, evidencing the vital role of the grain boundaries present in an otherwise continuous flake. This because of the interfacial stress transfer

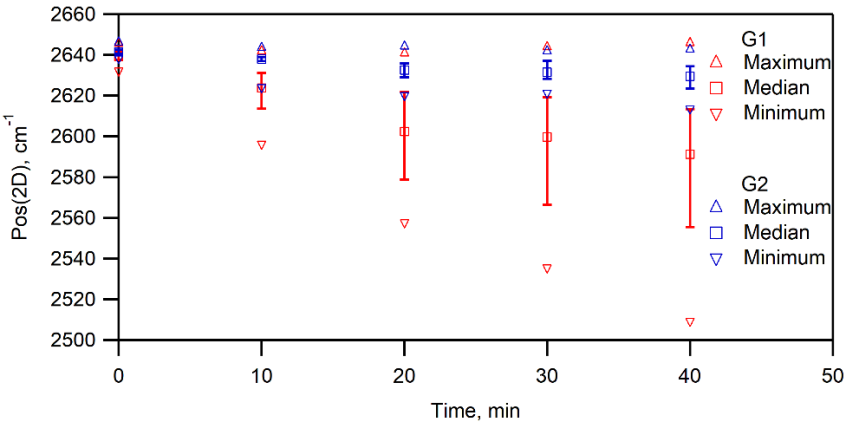

Figure 2. 2D band shift of the G1 and G2 graphene samples for different soaking periods.

failure at the edges of the graphene domains, i.e. boundaries [20]. The high stress-transfer in the sample G1 took place due to the absence of such boundaries.

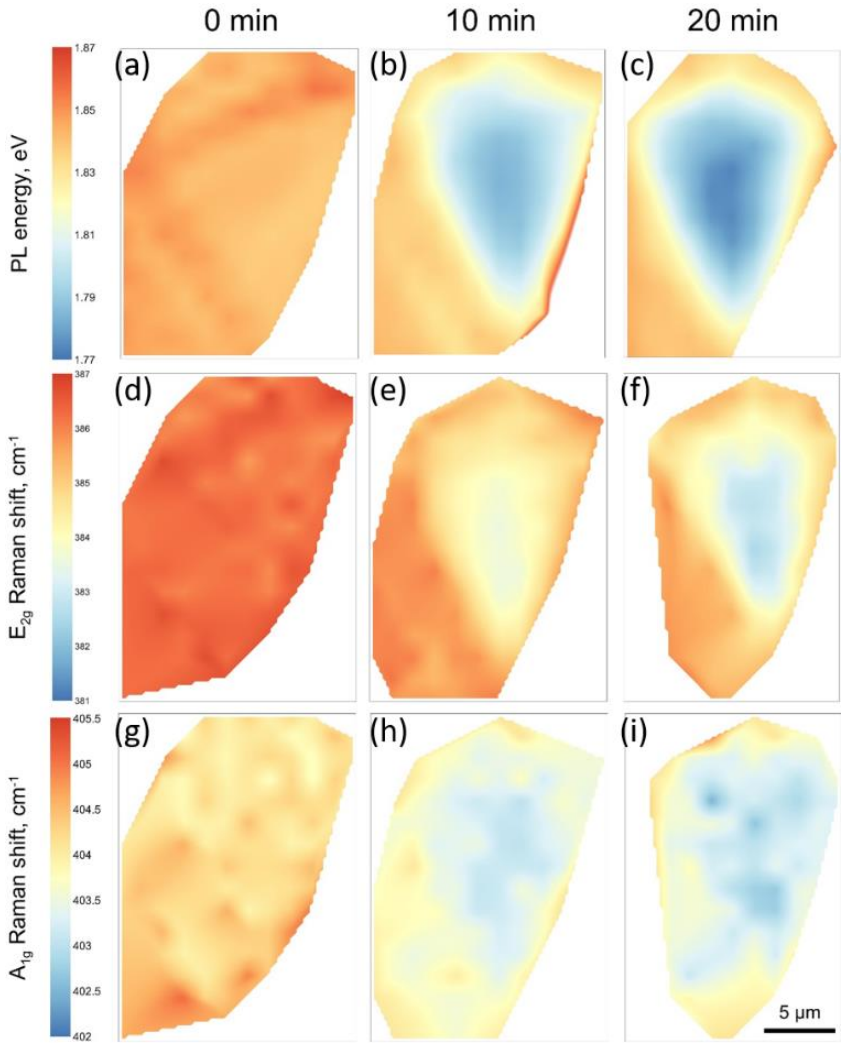

Figure 3.Evolution of PL and Raman spectral features of a monolayer MoS_2 sample. The shift in the color-coded (a-c) PL spectral map and Raman spectral map of E_{2g} (d-f) and A_1' (g-i) peaks for the different soaking period.

With the increasing soaking time, the extending size of the error bars in **Figure 2** for both G1 and G2 samples confirms the evolution of a strain gradient across the flakes. This evolution of the strain with the soaking time is evident as is the continuous strain gradient in the achieved biaxial strain on these atomically thin graphene layers [15,21].

We employ the same swelling technique to impose the biaxial strain on another 2D material, namely monolayer MoS_2. Since the MoS_2 has a different Raman signature than graphene, we considered the frequencies of the in-plane vibrational peak (E' or E_{2g}) at 386cm^{-1} and the out-of-plane vibrational peak (A_1') at 406 cm^{-1} to quantify the strain evolution in MoS_2. Besides the Raman modes, we employed the PL signal of the A exciton at ~1.88eV. The PL redshift as well as the Raman peaks' blue shift correspond to the tensile strain in the MoS2 sample [22,23].

The color-coded maps in **Figure 3 a-c** show the PL map of the MoS_2 flake as a response to the soaking times. To simplify the analysis, we treated both the A neutral exciton and trion as a single PL peak. **Figure 3 d-f** and g-i show the E' and A_1' peak shifts, respectively, as a result of the different soaking times [9]. As expected, the shift of the E' peak is larger than the shift of the A_1' peak for the given soaking time, due to the in-plane character of the E' mode and thus an increased sensitivity to an in-plane deformation. The stress transfer from the polymer to the MoS_2 flake failed after 20 minutes of soaking due to small size of the MoS_2 flake.

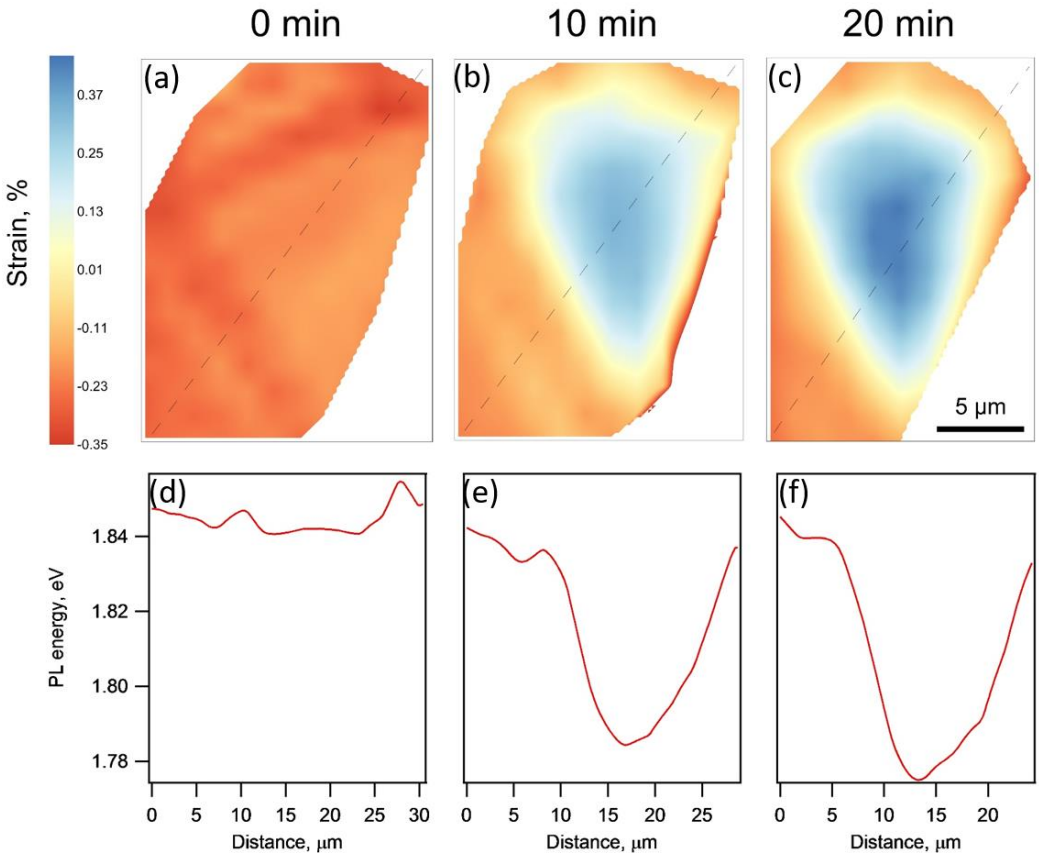

Figure 4 Evolution of biaxial strain quantified from the PL shift in MoS_2 for the different soaking times. (a-c) Maps of lattice deformation and (d-f) the corresponding PL shift from the profiles extracted diagonally, along the dashed lines in a-c.

Due to a relatively smaller strain-sensitivity of either of the Raman modes to small strains, PL A exciton peak was considered to quantify the imposed strain on the MoS_2 flake. Approximately maximum of 0.6% of biaxial strain was imposed on the center of the MoS_2 flake after 20 minutes of soaking time [23]. According to the Raman shifts, a potential change in charge-transfer doping during the experiment was negligible, as the ratio

of the E' and A_1' shifts corresponds to a pure effect of strain [24,25]. The profile across the color-coded PL spectral map in **Figure 4** shows the redshift in PL at different soaking times localized at the centre of the continuous MoS_2 flake where the highest strain was achieved. The profile extracted from **Figure 4 c** (i.e. **Figure 4 f**) shows the PL energy gradient forming a potential energy funnel imposed by the biaxial strain. Such an energy funneling, if even higher strain could be achieved as maxima, could be used in applications to power future devices [26-29].

4. CONCLUSION

We evidence that biaxial strain can be imposed on atomically thin monolayers of graphene and MoS_2 using the swelling of their polymer substrates by methanol. The Raman spectral shift of the 2D band was used to quantify the strain evolution in graphene, while in the case of MoS_2 also photoluminescence was employed. The stress transfer failed after 40 minutes of soaking time for graphene and after 20 minutes of soaking time for MoS_2. The different soaking time is due to the different sizes of the flakes or domains within. The large flake size can bear the more considerable biaxial deformation in the swelling experiment. The smaller flake size or more abundant sample boundaries fail to transfer the strain at an earlier soaking time. In both graphene and MoS_2, the biaxial strain is tensile corresponding to the volume swelling of the substrate. Hence, the MoS_2 band gap energy was decreased as the effect of the imposed biaxial strain, and the median strain level achieved was 0.5% in both graphene and MoS_2.

ACKNOWLEDGEMENTS

We acknowledge the support of the Grant Agency of the Czech Republic under the contract GJ18-06498Y and the support of internal grant of CEITEC VUT/FEKT-J-20-6541.The support of the European Regional Development Fund; OP RDE; Project: "Carbon allotropes with rationalized nano interfaces and nano links for environmental and biomedical applications" (No. CZ.02.1.01/0.0/0.0/16_026/0008382) is also acknowledged.

REFERENCES

[1] GUINEA, F. Strain engineering in graphene. *Solid State Communications*. 2012; vol. 152, no. 15, pp. 1437-41.

[2] DENG, S., SUMANT, A.V., BERRY, V. Strain engineering in two-dimensional nanomaterials beyond graphene. *Nano Today*. 2018; vol. 22, pp. 14-35.

[3] SI C., SUN Z., LIU F. Strain engineering of graphene: a review. *Nanoscale*. 2016; vol. 8, no. 6, pp. 3207-17.

[4] SCIDÀ, A., HAQUE, S., TREOSSI, E., ROBINSON, A., SMERZI, S., RAVESI, S. et al. Application of graphene-based flexible antennas in consumer electronic devices. *Materials Today*. 2018, vol. 21, no. 3, pp. 223-30.

[5] ANDROULIDAKIS, C., KOUKARAS, E.N., SAMPATHKUMAR, K., PARTHENIOS, J., PAPAGELIS, K., FRANK, O. et al. Wrinkled Few-Layer Graphene as Highly Efficient Load Bearer. *ACS Applied Materials & Interfaces*. 2017; vol. 9, no. 31, pp. 26593-601.

[6] SHUNDO, A., HORI, K., PENALOZA, D.P., YOSHIHIRO, K., ANNAKA, M., TANAKA, K. Nonsolvents-induced swelling of poly(methyl methacrylate) nanoparticles. *Physical Chemistry Chemical Physics*. 2013, vol. 15, no. 39, p.16574.

[7] SAUNDERS, J.E., CHEN, H., BRAUER, C., CLAYTON, M., CHEN, W., BARNES, J.A., et al. Quantitative diffusion and swelling kinetic measurements using large-angle interferometric refractometry. *Soft Matter*. 2015, vol. 11, no. 45, pp. 8746-57.

[8] KIM, H-N, KANG, J-H, JIN, W-M, MOON, J.H. Surface modification of 2D/3D SU-8 patterns with a swelling–deswelling method. *Soft Matter*. 2011, vol. 7, no. 6, pp.2989-93.

[9] HE, X., LI, H., ZHU, Z., DAI, Z., YANG, Y., YANG, P. et al. Strain engineering in monolayer WS2, MoS2, and the WS2/MoS2 heterostructure. *Applied Physics Letters*. 2016, vol. 109, no. 17, p. 173105.

[10] MUELLER, N.S., HEEG, S., ALVAREZ, M.P., KUSCH, P., WASSERROTH, S., CLARK, N. et al. Evaluating arbitrary strain configurations and doping in graphene with Raman spectroscopy. *2D Materials*. 2017, vol. 5, no. 1, p. 015016.

[11] WOUTERS, K., PUERS, R. Diffusing and swelling in SU-8: insight in material properties and processing. *Journal of Micromechanics and Microengineering*. 2010, vol. 20, no. 9, p. 095013.

[12] PAPANU, J.S., HESS, D.W., SOANE, (SOONG) D.S., BELL, A.T. Swelling of poly(methyl methacrylate) thin films in low molecular weight alcohols. *Journal of Applied Polymer Science*. 1990, vol. 39, no. 4, pp. 803-23.

[13] YI, L., XIAODONG, W., CHONG, L., ZHIFENG, L., DENAN, C., DEHUI, Y. Swelling of SU-8 structure in Ni mold fabrication by UV-LIGA technique. *Microsystem Technologies*. 2005, vol. 11, no. 12, pp.1272-5.

[14] JIE, W., YU HUI Y., ZHANG, Y., PING, LAU S, HAO, J. Effects of controllable biaxial strain on the Raman spectra of monolayer graphene prepared by chemical vapor deposition. *Applied Physics Letters*. 2013, vol. 102, no. 22, p. 223112.

[15] ZABEL, J, NAIR, R.R., OTT, A., GEORGIOU, T., GEIM, A.K., NOVOSELOV, K.S. et al. Raman Spectroscopy of Graphene and Bilayer under Biaxial Strain: Bubbles and Balloons. *Nano Letters*. 2012, vol.12, no. 2, pp. 617-21.

[16] BOUSIGE, C., BALIMA, F., MACHON, D., PINHEIRO, G.S., TORRES-DIAS, A., NICOLLE, J. et al. Biaxial Strain Transfer in Supported Graphene. *Nano Letters*. 2017, vol. 17, no. 1, pp. 21-7.

[17] TSOUKLERI, G., PARTHENIOS, J., PAPAGELIS, K., JALIL, R., FERRARI, A.C., GEIM, A.K. et al. Subjecting a Graphene Monolayer to Tension and Compression. *Small*. 2009, vol. 5, no. 21, pp. 2397-402.

[18] ANDROULIDAKIS, C., KOUKARAS, E.N., PARTHENIOS, J., KALOSAKAS, G., PAPAGELIS, K., GALIOTIS, C. Graphene flakes under controlled biaxial deformation. *Scientific Reports*. 2016, vol. 5, no. 1, p. 18219.

[19] SAMPATHKUMAR, K., DIEZ-CABANES, V., KOVARICEK, P., DEL CORRO, E., BOUŠA, M., HOŠEK, J. et al. On the Suitability of Raman Spectroscopy to Monitor the Degree of Graphene Functionalization by Diazonium Salts. *The Journal of Physical Chemistry C*. 2019, vol. 123, no. 36, pp. 22397-402.

[20] ANAGNOSTOPOULOS, G., ANDROULIDAKIS, C., KOUKARAS, E.N., TSOUKLERI, G., POLYZOS, I., PARTHENIOS, J. et al. Stress Transfer Mechanisms at the Submicron Level for Graphene/Polymer Systems. *ACS Applied Materials & Interfaces*. 2015, vol. 7, no. 7, pp. 4216-23.

[21] FU, X., SU, C., FU, Q., ZHU, X., ZHU, R., LIU, C. et al. Tailoring Exciton Dynamics by Elastic Strain-Gradient in Semiconductors. *Advanced Materials*. 2014, vol. 26, no. 16, pp. 2572-9.

[22] PAN, H., ZHANG, Y-W. Tuning the electronic and magnetic properties of MoS2 nanoribbons by strain engineering. *The Journal of Physical Chemistry C*. 2012, vol. 116, no. 21, pp. 11752-7.

[23] LLOYD, D., LIU, X., CHRISTOPHER, J.W., CANTLEY, L., WADEHRA, A., KIM, B.L., et al. Band Gap Engineering with Ultralarge Biaxial Strains in Suspended Monolayer MoS2. *Nano Letters*. 2016, vol. 16, no. 9, pp. 5836-41.

[24] KOU, L., DU, A., CHEN, C., FRAUENHEIM, T. Strain engineering of selective chemical adsorption on monolayer MoS 2. *Nanoscale*. 2014, vol. 6, no. 10, pp. 5156-61.

[25] MICHAIL, A., DELIKOUKOS, N., PARTHENIOS, J., GALIOTIS, C., PAPAGELIS, K. Optical detection of strain and doping inhomogeneities in single layer MoS2. *Applied Physics Letters.* 2016, vol. 108, no. 17, p.173102.

[26] CASTELLANOS-GOMEZ, A., ROLDÁN, R., CAPPELLUTI, E., BUSCEMA, M., GUINEA, F., VAN DER ZANT, H.S.J., et al. Local strain engineering in atomically thin MoS2. *Nano letters*. 2013, vol. 13, no. 11, pp. 5361-6.

[27] DING, Z., PEI, Q-X, JIANG, J-W, ZHANG, Y-W. Manipulating the thermal conductivity of monolayer MoS2 via lattice defect and strain engineering. *The Journal of Physical Chemistry C*. 2015, vol. 119, no. 28, pp. 16358-65.

[28] TYURNINA, A.V., BANDURIN, D.A., KHESTANOVA, E., KRAVETS, V.G., KOPERSKI, M., GUINEA, F. et al. Strained Bubbles in van der Waals Heterostructures as Local Emitters of Photoluminescence with Adjustable Wavelength. *ACS Photonics*. 2019, vol. 6, no. 2, pp.516-24.

[29] MOON, H., BERSIN, E., CHAKRABORTY, C., LU, A-Y, GROSSO, G., KONG, J. et al. Strain-Correlated Localized Exciton Energy in Atomically Thin Semiconductors. *ACS Photonics*. 2020, vol. 7, no. 5, pp. 1135-40.